

Order in driven vortex lattices in superconducting Nb films with nanostructured pinning potentials

M. Vélez^{a,*}, D. Jaque^a, J. I. Martín^{a,*}, F. Guinea^b, and J. L. Vicent^a

^a*Depto. Física de Materiales, F. Físicas, Universidad Complutense, 28040 Madrid, Spain*

^b*Instituto de Ciencia de Materiales de Madrid, CSIC, Cantoblanco, 28049 Madrid, Spain*

(November 6, 2018)

Abstract

Driven vortex lattices have been studied in a material with strong pinning, such as Nb films. Samples in which natural random pinning coexists with artificial ordered arrays of defects (submicrometric Ni dots) have been fabricated with different geometries (square, triangular and rectangular). Three different dynamic regimes are found: for low vortex velocities, there is a plastic flow regime in which random defects frustrate the effect of the ordered array; then, for vortex velocities in the range 1-100 m/s, there is a sudden increase in the interaction between the vortex lattice and the ordered dot array, independent on the geometry. This effect is associated to the onset of quasi long range order in the vortex lattice leading to an increase in the overlap between the vortex lattice and the magnetic dots array. Finally, at larger velocities the ordered array-vortex lattice interaction is suppressed again, in agreement with the behavior found in numerical simulations.

The influence of both applied magnetic field and driving current on the type II superconductors behavior is of great scientific and technological interest. When the vortex lattice is driven by an applied current in the presence of defects, it can adopt several dynamic flow regimes depending on the driving current and therefore on the vortex velocity. Transport measurements [1], neutron scattering [2] and Bitter decoration experiments [3,4] have provided strong evidence of these different dynamics phases, including creep, plastic flow and ordered (elastic) flow, and even of the existence of several phase transitions as a function of vortex velocity [5,6]. Due to this complex behavior, the vortex lattice emerges as an excellent model system for many interesting fields in condensed matter physics such as self-organized criticality, atomic scale friction and phase transitions in the presence of disorder/order [7,8].

Theoretical works on driven vortex lattices, in the presence of either random [9] or ordered [10,11] pinning centers, have predicted rich phase diagrams as a function of vortex velocity and pinning strength. In general, most of the experimental studies have focused on dynamic phases in the presence of weak random pinning centers in materials such as $2H$ -NbSe₂ single crystals [12] or amorphous Nb₃Ge films [13] where the low values of the critical current allow experimental access to a wide portion of the relevant force-velocity space. However, driven vortex lattices materials with strong pinning, such as Nb, have received much less attention. In these systems, the fabrication of ordered arrays of artificial pinning centers by submicrometric lithographic techniques have proved to be a very useful tool in the study of vortex dynamics under tailored nanostructured pinning potentials [14–18].

In particular, depending on the size and material of the artificial pinning centers, the relative strength of the ordered and disordered pinning potentials in the sample can be tuned in a controlled way [19].

In this work, we present results obtained from transport measurements on Nb films with ordered arrays of magnetic dots in order to study the dynamic interactions of the vortex lattice with random and ordered defects. Deformations in the vortex lattice frustrate the interactions with the artificial dot array for slow vortex motion, until the onset of ordering in the vortex lattice takes place for vortex velocities in the 1-10 m/s range. The evidence of this transition has been found to be independent on array geometry, indicating that the ordered array of dots is acting as a probe of the intrinsic behavior of the driven vortex lattice. Finally, for velocities above 100 m/s the effect of the ordered array on the moving vortex lattice disappears, in good agreement with numerical simulations.

Magnetic (Ni) dots approximately 200 nm in diameter and 40 nm in thickness were prepared on Si(100) substrates using electron beam lithography combined with a lift-off process described elsewhere [15,20]. After this, a 100 nm thick Nb film was sputtered on top. Finally optical lithography and reactive ion etching were used to define a 80 μm wide bridge for transport measurements. Three different array geometries were fabricated: $0.45 \times 0.45 \mu\text{m}^2$ square array, $0.35 \times 0.5 \mu\text{m}^2$ rectangular array and a triangular array with a lattice constant of 0.4 μm .

In the case of the rectangular array, transport measurements were carried out by applying current parallel to the shortest lattice dimension. The dc measurements were performed in a helium cryostat with a 9T superconducting magnet. The magnetic field is always applied along the film normal.

As a first approach to the dynamics of driven vortex lattices we can consider that, in the presence of a driving current, the vortex lattice is set into motion with average velocity \mathbf{v}

by the Lorentz force $\mathbf{F}_L = \Phi_0 \mathbf{J} \times \mathbf{n}$, where \mathbf{J} is the transport current, Φ_0 is the quantum of flux, and \mathbf{n} is the unit vector along the field direction. The vortex velocity \mathbf{v} is determined by the balance between the viscous, pinning and Lorentz forces as [21]

$$\eta \mathbf{v} + \alpha \mathbf{v} \times \mathbf{n} = \mathbf{F}_L + \langle \mathbf{F}_P \rangle \quad (1)$$

where η is the Bardeen-Stephen viscosity, α is the viscous Hall coefficient, and $\langle \mathbf{F}_P \rangle$ is the pinning force averaged over vortex positions in time. In the dirty limit, $\alpha \ll \eta$ and the viscous Hall force can be neglected. The resulting force-velocity curves (F_L vs v) can be simply derived from experimental I-V characteristics calculating the Lorentz force and using the Josephson relation for the electric field $\mathbf{E} = \mathbf{B} \times \mathbf{v}$, as shown in Fig. 1 for a Nb film with and without periodic pinning centers. For low velocities the curves approach a constant force value that corresponds to the static pinning force F_{P0} , related to the critical current J_C by $F_{P0} = \Phi_0 J_C$. The free flux flow behavior, characterized by a linear dependence of F_L on v should be recovered for very high velocities, where the interaction between the pinning centers and the vortex lattice becomes negligible. However pure free flux flow is usually only accessible experimentally by fast ramp current methods, even in relatively weak pinning materials [22]. Often, in a wide range of vortex velocities such as plotted in Fig.1, the force velocity dependence is found to be much weaker than linear, revealing that the term corresponding to pinning interactions $\langle \mathbf{F}_P \rangle$ is of the same order as the Bardeen-Stephen viscous force.

The calculation of $\langle \mathbf{F}_P \rangle$ is not straightforward, since interactions among the vortices and with the pinning centers induce dynamic deformations in the vortex lattice that strongly affect this average. The orientation of $\langle \mathbf{F}_P \rangle$ is opposite to the vortex velocity [21], i.e. it can be written as $\langle \mathbf{F}_P \rangle = -\gamma(v) \hat{\mathbf{v}}$, with $\gamma(v)$ a velocity dependent coefficient and $\hat{\mathbf{v}}$ the unit vector along \mathbf{v} . At sufficiently large driving currents, the time average of the pinning force is related to the spatial average by $\langle \mathbf{F}_P \rangle_{\text{time}} \approx \langle |\mathbf{F}_P|^2 \rangle_{\text{position}} / |\mathbf{v}|$. The equation of motion of the vortex lattice is given by

$$\eta \mathbf{v} + \gamma(v) \hat{\mathbf{v}} = \mathbf{F}_L \quad (2)$$

Equation (2) implies that the effect of pinning centers can be assimilated to a kinetic viscous force, in a similar way to the problem of friction between two solids [8] (in this case, the vortex lattice and the pinning array).

The distribution and strength of the pinning centers affect both the magnitude and velocity dependence of $\langle \mathbf{F}_P \rangle$. This is clearly observed, for example, in differences between the two $F_L - v$ curves in Fig.1, that were measured in two adjacent regions of the same Nb film, with and without periodic pinning centers. Further insight in the behavior of the vortex lattice can be obtained by focusing on the differences in $\langle \mathbf{F}_P \rangle$ depending on the commensurability between the vortex lattice and periodic array of dots.

A general view of the effect of commensurability is shown in Fig.2, where we have plotted the voltage versus magnetic field curves obtained for different current densities in the range $10^7 - 10^9$ A/m² for the Nb film with the square array of magnetic dots. Magnetoresistance minima are observed at equal magnetic field intervals, $\Delta H_m = 98$ Oe. These can be explained [15] by a geometric matching between the vortex lattice and the magnetic dot array. It should be noted that the current dependence of the magnetoresistance is not the same whether the measuring field corresponds to a matching condition or not. These differences show up in

the fact that the magnetoresistance minima are much deeper in an intermediate current range than at low and high currents. Actually, the critical current, shown in the inset of Fig.2, presents a monotonous decrease as a function of field, without any special feature at the matching field values. These magnetoresistance and critical current data are clearly indicating the existence of several different regimes: first, at $v = 0$, the static pinning force F_{P0} is dominated by the random pinning centers, that frustrate the effect of the ordered array of dots; then, in the driven vortex lattice the kinetic viscous force due to the ordered array of pinning centers $\langle \mathbf{F}_P \rangle$ is enhanced in a certain velocity range, and disappears at large driving currents. This behavior is characteristic of small dot diameter arrays where periodic pinning is weaker than random pinning, and it is also observed for the rectangular and triangular arrays used in this study, but with $\Delta H_m = 120$ and 145 Oe, respectively, in good agreement with theoretical predictions of the matching conditions.

Figures 3(a)-(c) show the force-velocity curves in the driving current range where commensurability minima are observed, derived from the I-V characteristics, for the Nb films with square, triangular and rectangular arrays of dots measured at two different fields: at the first matching field H_{comm} for each array (filled symbols) and at a smaller field value H_{incomm} close to H_{comm} but far enough to be out of matching conditions (hollow symbols). The obtained curves present quite similar values for low and high vortex velocities. At intermediate vortex velocities (1-100 m/s) the matching curve differs from that obtained at non matching fields. In all cases, the overall dependence is clearly weaker than linear, indicating that the vortex lattice is far from the free flux flow regime. Two kinds of force contributions can be considered in this system; the sum of the Bardeen-Stephen viscous force and the interaction with random defects ($\eta v + \langle F_{P,random} \rangle$), and the average interaction force from the periodic array $\langle F_{P,ordered} \rangle$, which is a strongly peaked function of the magnetic field at the matching condition. In a first approximation, taking into account that in these samples random pinning is much stronger than periodic pinning, $\langle F_{P,ordered} \rangle$ can be assumed to be negligible for the incommensurate vortex lattice; then the difference between the filled and hollow symbols curves can be used to extract the value of $\langle F_{P,ordered} \rangle$ at the matching conditions.

This force increment, $\Delta F = F(H_{comm}) - F(H_{incomm}) = \langle F_{P,ordered} \rangle$ is shown in Figs. 3(d)-(f) for the three arrays considered in this work. There is a clear onset of the interactions with the ordered pinning array in the range 1-10 m/s, observable in the three cases. This onset is almost independent on the ordered array geometry, so that it must be related with an intrinsic change in the properties of the driven vortex lattice. The increase in $\langle F_{P,ordered} \rangle$ can be directly correlated with an enhancement in the long range order in the vortex lattice, since this force should be zero for a completely disordered vortex state. Therefore, the data in Fig. 3 show the crossover between two different regimes: first, for slow vortex motion $\langle F_{P,ordered} \rangle = 0$, implying a plastic motion regime where the effect of the ordered array is frustrated by random pinning and, then, for $v \sim 10$ m/s the lattice flows in a more ordered state in which it has a better overlap with the magnetic dot array.

In general, theoretical simulations of driven vortex lattices have predicted [9,10] two kinds of ordered states: a smectic glass phase, with quasi long range order only in the direction transverse to the motion, and a Bragg glass phase at higher velocities that is also ordered along the longitudinal direction. It is worth to note that the ordered pinning effect observed here occurs at H_{comm} corresponding to matching between the vortex lattice with the two

dimensional dot array cell (this is particularly evident in the case of the rectangular array, where $H_{comm} = 120$ Oe corresponds to a vortex density $5.8 \times 10^8 \text{ cm}^{-2}$ in good agreement with the density of pinning centers $(0.35 \times 0.5 \mu\text{m}^2)^{-1} = 5.7 \times 10^8 \text{ cm}^{-2}$). This implies that both the longitudinal and transverse correlation lengths in the vortex lattice are at least as large as the array cell dimension when the peak in ΔF appears, suggesting the presence of a Bragg glass phase. The ordering velocity that we have found in these Nb films is two orders of magnitude higher than those obtained previously for other superconducting systems [22] such as $2H\text{-NbSe}_2$ (typically of the order of 0.1 m/s). These differences can be correlated with the higher values of the critical current in our samples that imply stronger random pinning potentials ($J_C \approx 10^7 \text{ A/m}^2$ in the Nb films presented in this work, while $J_C \approx 10^5 \text{ A/m}^2$ in [22]).

Finally, it has to be noted that for vortex velocities above 100 m/s, ΔF decreases again, i.e. the interaction between the ordered array and the vortex lattice is suppressed. We have tried to understand this large velocity regime by modelling the moving vortex lattice by a 1D array of point particles which move under a driving force in a combination of a periodic potential and random pinning centers. A similar setup, in 2D, was considered in [8], although the issue of commensurability was not addressed. Our model is an approximation to the 1D chains with short range order which are expected in a driven smectic [23]. The results are shown in Fig.4. Commensurability effects appear only at one matching field, due probably to the length of the chain used (20-30 vortices). It is interesting to note that, as in the experimental data shown in Fig.2, these effects disappear at large driving currents. The simulations show that there are, at least, three different regimes: i) At low driving currents, the lattice remains disordered at all fields, leading to structureless V-B curves. ii) At intermediate currents, the vortex lattice shows some degree of order, which increases as a function of the field. In this regime the minimum in the V-B curves at the matching field is most pronounced. iii) Finally, at high driving currents, the lattice is very well ordered, with no substantial dependence on the applied field. In this regime, the effects at H_{comm} are very weak, if any. It is worth to note that the same effect of reduction in the interaction force at high velocities has been numerically predicted in simulations of the similar problem of friction between two lattices at atomic scale [8].

In summary, we have analyzed the force-velocity characteristics for several Nb films with square, triangular and rectangular arrays of Ni dots, in which ordered and disordered defects coexist. By comparison of the curves at matching magnetic field and away from matching conditions we have found that there is a clear increase in the interactions between the vortex lattice and the ordered array of dots in the vortex velocity range 1-100 m/s. The sudden enhancement in $\langle F_{P,ordered} \rangle$ has been attributed to the onset of quasi long range order in the vortex lattice at this driving velocity. This result is independent on the array geometry, indicating that a change in the intrinsic properties of the vortex lattice is being observed. For very high vortex velocities, commensurability effects are suppressed again, in agreement with numerical simulations.

ACKNOWLEDGMENTS

This work has been supported by the Spanish CICYT (grant MAT99/0724, and PB96/0875) and by the European Science Foundation VORTEX program. We thank G.

W. Crabtree for useful comments.

REFERENCES

- * Present address: Depto. Física, Universidad de Oviedo, Spain.
- [1] S. Battacharya and M. J. Higgins, Phys. Rev. Lett. **70** 2617 (1993).
 - [2] U. Yaron, P. L. Gammel, D. A. Huse, R. N. Kleiman, C. S. Oglesby, E. Bucher, B. Batlogg, D. J. Bishop, K. Mortensen, K. Clausen, C. A. Bolle and F. de la Cruz, Phys. Rev. Lett. **20**, 748 (1994)
 - [3] F. Pardo, F. de la Cruz, P. L. Gammel, E. Bucher and D. J. Bishop, Nature **396**, 6709 (1998).
 - [4] M. Marchevsky, J. Aarts and P. H. Kes, Phys. Rev. B **60**, 14601 (1999).
 - [5] A. E. Koshelev and V. M. Vinokur, Phys. Rev. Lett. **73**, 3580 (1994)
 - [6] L. Balents and M. P. A. Fisher, Phys. Rev. Lett. **75**, 4270 (1995).
 - [7] K. E. Bassler and M. Paczuski, Phys. Rev. Lett. **81**, 3761 (1998).
 - [8] T. Kawaguchi and H. Matsukawa, Phys. Rev. B **61**, R16366 (2000).
 - [9] P. L. Doussal and T. Giamarchi, Phys. Rev. B **57**, 11356 (1998).
 - [10] C. Reichhardt, C. J. Olson, and F. Nori, Phys. Rev. B **58**, 6534 (1998); C. Reichhardt and G. T. Zimanyi, Phys. Rev. B **61**, 14354 (2000).
 - [11] V. M. Marconi and D. Dominguez, Phys. Rev. Lett. **82**, 4922 (1999).
 - [12] W. Henderson, E. Y. Andrei, M. J. Higgins and S. Battacharya, Phys. Rev. Lett. **80**, 381 (1998).
 - [13] P. Berghuis, A. L. F. van der Slot and P. H. Kes, Phys. Rev. Lett. **65**, 2583 (1990).
 - [14] M. Baert, V. V. Metlushko, R. Jonckheere, V. V. Moshchalkov and Y. Bruynseraede, Phys. Rev. Lett. **74**, 3279 (1995).
 - [15] J. I. Martín, M. Vélez, J. Nogués, and I. K. Schuller, Phys. Rev. Lett. **79**, 1929 (1997).
 - [16] D. J. Morgan and J. B. Ketterson, Phys. Rev. Lett. **80**, 3614 (1998).
 - [17] J. I. Martín, M. Vélez, A. Hoffmann, I. K. Schuller and J. L. Vicent, Phys. Rev. Lett. **83**, 1022 (1999).
 - [18] V. Metlushko, U. Welp, G. W. Crabtree, R. Osgood, S. D. Bader, L. E. DeLong, Z. Zhang, S. R. J. Brueck, B. Ilic, K. Chung, and P. J. Hesketh, Phys. Rev. B. **60**, R12585 (1999).
 - [19] A. Hoffmann, P. Prieto and I. K. Schuller, Phys. Rev. B **61**, 6958 (2000).
 - [20] J. I. Martín, Y. Jaccard, A. Hoffmann, J. Nogués, J. M. George, J. L. Vicent, and I. K. Schuller, J. Appl. Phys. **84**, 411 (1998).
 - [21] V. M. Vinokur, V. B. Geshkenbein, M. V. Feigel'man and G. Blatter, Phys. Rev. Lett. **71**, 1242 (1993).
 - [22] Z. L. Xiao, E. Y. Andrei, P. Shuk and M. Greenblatt, Phys. Rev. Lett. **85**, 3265 (2000).
 - [23] L. Balents, M. C. Marchetti and L. Radzihovsky, Phys. Rev. B **57**, 7705 (1998).

FIG. 1. Force vs velocity curves derived from the I-V characteristics for (a) a simple Nb film and (b) a Nb film on a rectangular array of Ni dots, grown on the same substrate, at $H = 81$ Oe and $T = 0.98T_C$. This field corresponds to the first matching field of the rectangular array.

FIG. 2. (a) $V - B$ curves obtained on the square array at $T = 0.99T_C$ for different current densities ($J = 6.25 \times 10^6, 1.25 \times 10^7, 3.1 \times 10^7, 6.25 \times 10^7, 9.4 \times 10^7, 1.25 \times 10^8, 1.56 \times 10^8$ and $1.87 \times 10^9 A/m^2$ for the (a)-(h) curves respectively). Inset shows the field dependence of the critical current at the same temperature.

FIG. 3. (a) Force-velocity characteristics for (a) a Nb film on a $0.45 \times 0.45 \mu m^2$ square array of dots (filled symbols, $H_{comm} = 98$ Oe; hollow symbols, $H_{incomm} = 60$ Oe) (b) a Nb film on a triangular array of dots of lattice constant $0.4 \mu m$ (filled symbols, $H_{comm} = 145$ Oe; hollow symbols, $H_{incomm} = 114$ Oe) (c) a Nb film on a $0.35 \times 0.5 \mu m^2$ rectangular array of dots (filled symbols, $H_{comm} = 120$ Oe; hollow symbols, $H_{incomm} = 90$ Oe); (d), (e), (f) Force increment $\Delta F = F(H_{comm}) - F(H_{incomm})$ (i.e. from no matching conditions to matching conditions) as a function of vortex velocity for the Nb films in (a), (b) and (c) respectively. Lines are guides to the eye.

FIG. 4. $V - B$ characteristics of a model of moving vortices under the influence of a periodic potential and random pinning (see text), corresponding to: filled symbols, $J = 10J_0$ and hollow symbols, $J = 2.5J_0$, where J_0 is the critical current at $0.6 H_{comm}$.

FIGURES

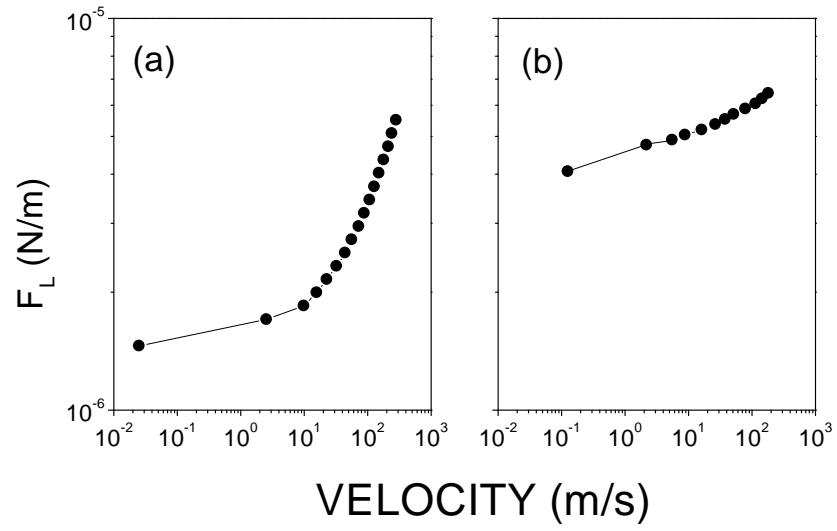


FIG. 1. M. Velez et al.

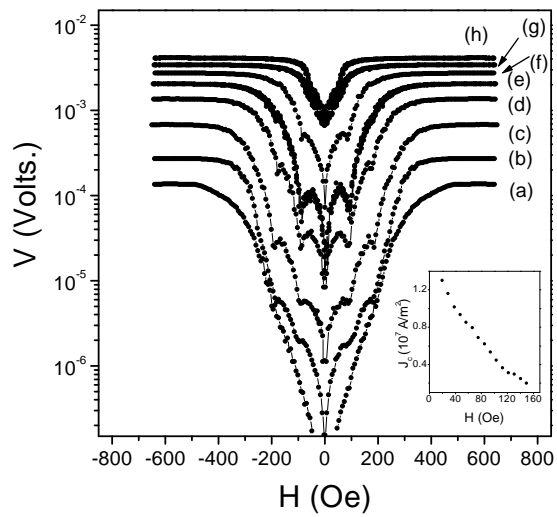


FIG. 2. M. Velez et al.

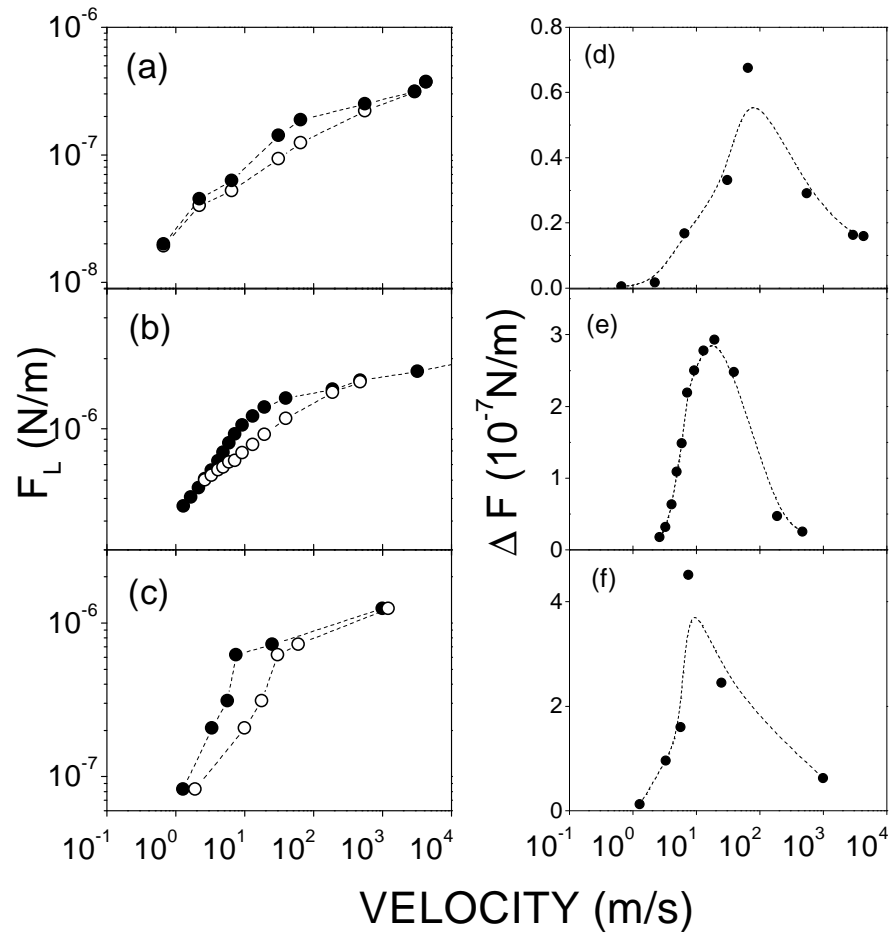


FIG. 3. M. Velez et al.

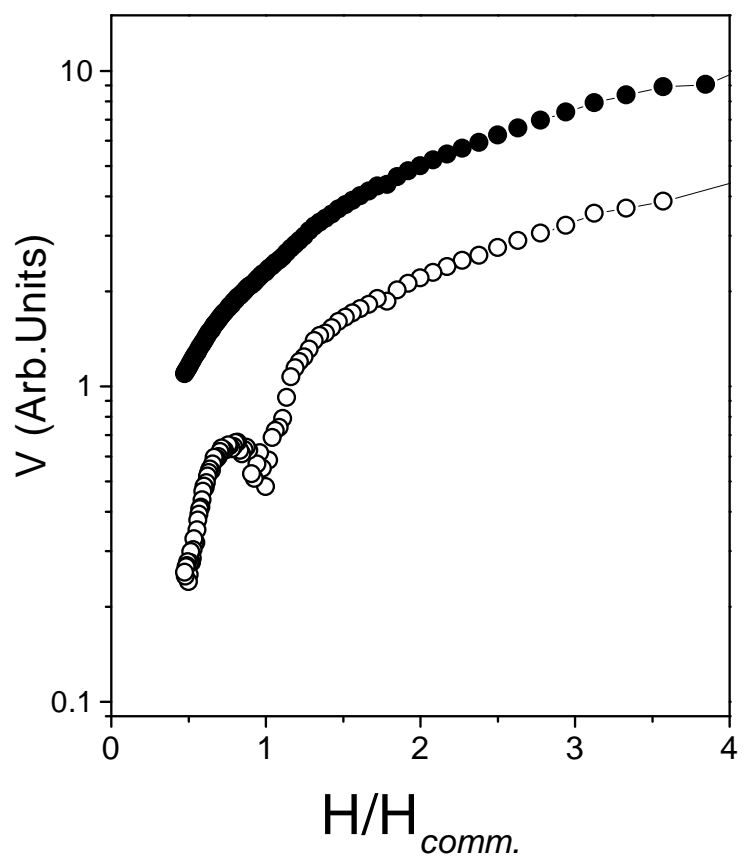


FIG. 4. M. Velez et al.